RPE Radiation Physics & Engineering
An International Peer-Reviewed Journal
Published by K.N. Toosi University of Technology
http://rpe.kntu.ac.ir
Research Article

Radiation Physics and Engineering 2020; 1(2):13–21
https://doi.org/10.22034/RPE.2020.63477

# Study of PWR transients by coupling of ANSYS-CFX with a kinetic model

Hossein Sharifian, Mahdi Aghaie*, Ahmad Zolfaghari
*Nuclear Engineering Department, Shahid Beheshti University, G.C, P.O. Box 1983963113, Tehran, Iran*

HIGHLIGHTS

- The reactivity response of an irradiated PWR core with coupling CFX and PKM is studied.
- Effects of fission gas release, dissolved gases, porosity, radiation damage and fuel Burnup are considered.
- Using the MMS, the online data transferring from CFX and subroutines is available.
- The response of the BNPP reactor in several reactivity insertions during burnups is studied.
- The effects of irradiation on dynamic response of fuel in a FA and core are shown.

ABSTRACT

In this work, dynamic responses of a WWER-1000 reactor in reactivity insertions are studied using a coupling method. The ANSYS-CFX is implemented for thermal hydraulic study of the core and the point kinetic equation (PKE) is coupled as a FORTRAN subroutine. For transient analysis of the core, the thermal feedback of the fuel is added to coolant, and numerical solver of cylindrical heat transfer for obtaining the irradiated fuel rod temperature profile is also included. In order to investigate the irradiation effect, the fuel and gap properties in burnup with appropriate correlations could be calculated. Using memory management system (MMS) and data transfer arrays, coupling between numerical subroutines is carried out. It is shown that the dynamic response of the core depends on burnup, and the response could be varied in time. In addition, the coupling method is reliable for other dynamic calculations.

KEYWORDS
WWER-1000
CFD
ANSYS-CFX
Burnup
Point Kinetic Model

HISTORY
Received: 2 October 2017
Revised: 9 March 2018
Accepted: 9 April 2018
Published: June 2020

## 1 Introduction

In recent decades, dynamic simulation is extended by two principal purposes: control of systems to exploit normal operation near the steady state situations, and creating appropriate gadgets to observe and to forecast variables which vary at events, emergency situations and system equipment failure (Luyben, 2012). The Dynamic Simulator for Nuclear Power Plants (DSNP) is similar to the commercial codes, and has therefore been directly designed according to reactor system diagrams and their behaviors. It is possible to change, add or define equations to better describe the system for simulation (Aghaie et al., 2012). According to the theories exhibited by Olander (Olander, 1976), the recommend of solid fission products into the nuclear fuel should show a small decrease in the thermal conductivity. The burnup effects could be calculated on the solid conductivity by considering some parameters such as build dissolved and precipitated fission products into the matrix (FD), the effect of the precipitated fission products (FP), porosity (FM) and radiation effects (FR). In addition, considering the effects of burnup on the gap conductivity and on the mixture property as well, correction of the fuel temperature in different burnup is possible.

Utilizing an appropriate software for simulation of specific requirements of a system is an important challenge. Thermo-hydraulic study in the nuclear industry needs high accuracy for solutions. Moreover, the boundary conditions and environmental system situation should be taken into account. In simulation of nuclear systems, particular codes with certain limits are generally used. They have been usually written in one dimensional, are closed source, and do not satisfy all the user's requirements. In addition, the fluid simulation in one dimension can not fully describe its behavior. By growing the computer technology and development of new capabilities, multi-dimensional computational fluid dynamics (CFD) has been extremely developed. By developing this type of simulations, the International Atomic Energy Agency (IAEA) reported the current and future role of CFD software for checking the safety problems of nuclear reactors

*Corresponding author: M_Aghaie@sbu.ac.ir

(Smith, 2010). Multi-dimensional simulation softwares designed so far are not primarily for using in the nuclear industry and do not support the related equations.

Considering the points mentioned, finding a method which provides using nuclear codes for checking the behavior of neutronics systems and for concurrent coupling the multi-dimensional simulation software to check the fluid action can be the solution of many similar problems. This method has been used to check the safety of liquid metal fast reactors, by coupling point kinetic equation (PKE) and PTM equations to Fluent software to be used in an unprotected transient over-power incident (Chen et al., 2015). The other way is coupling Dyn3D and Athlet neutron kinetics codes with FLUENT software to simulate breaking a cooling pipe in a WWER-1000 reactor (Vyskocil and Macek, 2014). The purpose of the current work is the use of the CFX simulation software which shows a relatively high convergence in the transient physical questions compared with Fluent, arisen from the utilization of coupling solver methods. Furthermore, owing to the fact that most nuclear codes are written using FORTRAN programming language, coupling with subroutines written using this language would be available.

According to these points, this paper attempts to simulate the behavior of fuel assemblies of a WWER-1000 reactor in the different fuel burnup in transient situations using the CFX software to add required nuclear equations such as presented heat transfer equations in the fuel rods and appending PKE equation. This method makes the evaluation of different transient possible.

## 2 Governing equations

The parameters and constants used in the following equations are defined in Table 1.

### *2.1 Point kinetics model*

The point kinetic equations are a coupled set of ordinary differential equations. They include six groups of delayed neutrons. A set of seven coupled differential equations will therefore be appeared:

$$\frac{\mathrm{d}n}{\mathrm{d}t} = (\frac{\rho - \beta}{\Lambda})n + \sum_{i=1}^{6} \lambda_i C_i + s \tag{1}$$

$$\frac{\mathrm{d}C_i}{\mathrm{d}t} = \frac{\beta_i}{\Lambda} n - \lambda_i C_i \qquad i = 1, ..., 6 \tag{2}$$

Because of complexity of the problem, analytical solutions are not usually available and using the numerical methods are therefore proposed. In the current work, the Runge-Kutta fourth order method is used. Runge-Kutta is a method for numerically integrating ordinary differential equations and therefore can be considered as relative of implicit and explicit Euler methods. This model is added to the CFX by a FORTRAN subroutine.

### *2.2 Thermal calculations*

#### 2.2.1 Fuel pellet temperature profile

For calculating heat transfer and temperature profile in the fuel pellet, the general equations of heat conduction in the cylindrical coordinate could be used:

$$\frac{1}{r}\frac{\mathrm{d}}{\mathrm{d}r}[rk_{fuel}(r)\frac{\mathrm{d}T_{fuel}}{\mathrm{d}r}] + q^{'''} = 0 \tag{3}$$

Hence, the analytical solutions by implementing boundary and initial conditions can be simplified to Eq. (4):

$$T(r) = \frac{q^{'''}}{4k_{ave}}(r^2 - r_{fs}^2) + T_{fs} \tag{4}$$

#### 2.2.2 Zircaloy clad temperature drop

For calculating heat transfer and temperature dropping in the clad, the Fourier's law could be used. Fourier's law presents the time rate of heat transfer via a parameter which is proportional to the ratio of the temperature to the direction of that gradient:

$$q = -kA\frac{\mathrm{d}T}{\mathrm{d}r} \tag{5}$$

Temperature through cylindrical shells can be changed to the integral form of Fourier's law as shown by Eq. (6):

$$T(r) = T_a + \frac{\ln(\frac{r}{r_a})}{\ln(\frac{r_b}{r_a})}(T_b - T_a) \tag{6}$$

#### 2.2.3 Gap temperature drop

The fuel-cladding gap temperature drop is calculated by using the fuel rod surface heat flux at altitude and the fuel-cladding gap conductance:

$$\Delta T_{gap} = \frac{q''(z)}{h}, \qquad h = h_{rad} + h_{gas} + h_{solid} \tag{7}$$

The fuel-cladding gap conductance is the sum of three components: the conductance due to radiation, the conduction through the gas, and the conduction through regions of solid-solid contact (Berna et al., 1997). The equations and models for each of these components are presented in different basis.

### *2.3 Thermal conductivity of irradiated material*

#### 2.3.1 Fuel pellet thermal conductivity

The used fuel thermal conductivity is based on the expression developed by Lucuta *et al.* (Lucuta et al., 1996). This expression, shown in Eq. (8), includes the term for the conductivity of unirradiated fuel and four different factors for its correctiion:

$$k_{un\_irr} = \frac{1}{0.0375 + 2.165 \times 10^{-4}T} + (\frac{4.715 \times 10^9}{T^2}) \times \exp(-\frac{16361}{T}) \tag{8}$$

**Table 1:** List of the parameters and constants used in this work.

| Parameter | Definition | Parameter | Definition |
|---|---|---|---|
| $A$ | Surface ($m^2$) | $r_b$ | Clad inner radius (m) |
| $B$ | Burnup (MWd/KgU) | $s$ | Shape factor |
| $C_i$ | Delayed neutron precursor concentration group $i$ | $T(r)$ | Temperature of intended point (K) |
| $h$ | Gap conductance ($W/m^2$-K) | $T_{fuel}$ | Fuel temperature (K) |
| $h_{rad}$ | Conductance due to radiation ($W/m^2$-K) | $T_{fs}$ | Outer fuel temperature (K) |
| $h_{gas}$ | Conductance of the gas gap ($W/m^2$-K) | $T_a$ | Outer clad temperature (K) |
| $h_{solid}$ | Conductance contact ($W/m^2$-K) | $T_b$ | Inner clad temperature (K) |
| $k_c$ | Zircaloy (clad) thermal conductivity (kW/m-K) | $\Delta T_{gap}$ | Gap temperature change (K) |
| $k_{fuel}$ | Fuel thermal conductivity (W/m-K) | $t$ | Time (s) |
| $k_{ave}$ | Fuel average thermal conductivity (W/m-K) | $x_{He}$ | Helium atom fraction in gap |
| $k_{un\_irr}$ | Conductivity of unirradiated uranium (W/m-K) | $x_{Xe}$ | Xenon atom fraction in gap |
| $k_{He}$ | Helium thermal conductivity (kW/m-K) | $x_{Kr}$ | Krypton atom fraction in gap |
| $k_{Xe}$ | Xenon thermal conductivity (kW/m-K) | $\rho$ | Total or net reactivity |
| $k_{Kr}$ | Krypton thermal conductivity (kW/m-K) | $\Lambda$ | Effective prompt neutron generation time (s) |
| $k_{mix}$ | Gas mixture thermal conductivity (kW/m-K) | | |
| $n$ | Normalized fission power amplitude | $\beta$ | Total effective delayed-neutron fraction |
| $p$ | Porosity fraction | $\beta_i$ | Delayed-neutron fraction of isotope $i$ |
| $q$ | Heat (W) | $\lambda_i$ | Decay constant of isotope $i$ (1/s) |
| $q''(z)$ | Rod surface heat flux at elevation $z$ ($W/m^2$) | $FD$ | Effect of dissolved fission products into the matrix |
| $q'''$ | Power density of fuel ($W/m^3$) | | |
| $r$ | Radius of intended point (m) | $FP$ | Effect of the precipitated fission products |
| $r_{fs}$ | Fuel outer radius (m) | $FM$ | Effect of porosity |
| $r_a$ | Clad outer radius (m) | $FR$ | The radiation effect |

In order to take into account the irradiation effects in Eq. (8), some correction factors are introduced: FD is the correction factor for the effect of burnup due to dissolved and precipitated fission products into the matrix, FP is representative for the correction factor to reflect the precipitated fission products, FM shows the correction factor to consider the effect of porosity accounted by Maxwell factor, and finally, FR is the correction factor for radiation effect in the reactor. Eventually, Eq. (13) gives the thermal conductivity for irradiated uranium:

$$FD = \left[\frac{1.09}{B^{3.265}} + \frac{0.0643}{\sqrt{B}}\sqrt{T}\right] \times \arctan\left[\frac{1}{\frac{1.09}{B^{3.265}} + \frac{0.0643}{\sqrt{B}}\sqrt{T}}\right] \tag{9}$$

$$FP = 1 + \left[\frac{0.019B}{3 - 0.019B}\right]\left[\frac{1}{1 + \exp(-\frac{T - 1200}{100})}\right] \tag{10}$$

$$FM = \frac{1 - p}{1 + (s - 1)p} \tag{11}$$

$$FR = 1 - \frac{0.2}{1 + \exp(\frac{T - 900}{80})} \tag{12}$$

$$k = k_{un\_irr}(FD \times FP \times FM \times FR) \tag{13}$$

### 2.3.2 Zircaloy clad thermal conductivity

The thermal conductivity of Zircaloy clad is temperature dependent, as shown by Toebbe correlation:

$$k_c = 7.51 + (2.09 \times 10^{-2} \times T) - (1.45 \times 10^{-5} \times T^2) + (7.67 \times 10^{-9} \times T^3) \tag{14}$$

### 2.3.3 Gap thermal conductivity

By increasing the burnup over time, fission gases released arrived to the gap and would be mixed with helium. Since xenon and krypton constitute the largest part of the fission gases, they have properties different from those of helium. The thermal conductivity of this new mixture should be calculated. Properties of this mixture is proportional to the mole fraction of each one, which can be written as Eq. (18):

$$k_{He} = 3.366 \times 10^{-5} T^{0.668} \tag{15}$$

$$k_{Xe} = 4.0288 \times 10^{-8} T^{0.872} \tag{16}$$

$$k_{Kr} = 4.726 \times 10^{-8} T^{0.923} \tag{17}$$

$$k_{mix} = (k_{He})^{x_{He}} (k_{Xe})^{x_{Xe}} (k_{Kr})^{x_{Kr}} \tag{18}$$

## *2.4 CFD model*

ANSYS-CFX is one of the best computational fluid dynamics software, and is therefore employed to solve many of fluid flow simulations by trusty and precise solutions. The CFX program works based on “finite volume theory” and “finite element interpolation”, with “saved amounts in

computing nodes". Moreover, because of using the "coupled quasi-transient solver" method in stable physical conditions, provides an acceptable convergence and various turbulence models compared with other similar softwares.

## 3 Description of the coupling method

In this paper, the ANSYS-CFX is used as a fully three-dimensional CFD simulator in order to predict the coolant flow. For spatial modeling of fuel rods in reactor core, FORTRAN subroutines are implemented. These subroutines calculate the effects of burnup in rod material by changing the temperature.

According to Figs. 1 and 2, the simulation are performed through the following steps:

- At the first-time step and according to the fuel burnup, gap composition should be identified. The conduction heat transfer coefficient is then calculated for materials such as fuel, gap, and zirconium clad.
- The excess reactivity inserted is converted to the relative thermal power by point kinetic correlations to determine increasing or decreasing of the thermal power level in each fuel rod.
- Changing the coolant temperature in axial different areas is called by CFX commands and is stored in a specific variable.
- The fuel temperature is calculated in axial area corresponded to the coolant, in radial direction, and the average of the fuel temperature is saved in a variable.
- The reactivity due to temperature gradient in fuel and coolant in every area, calculated by temperature reactivity coefficient correlation, is considered as the system feedback.
- In each time step, thermal power coefficient is considered as the summation of system feedback and the excess reactivity, and this procedure repeats.

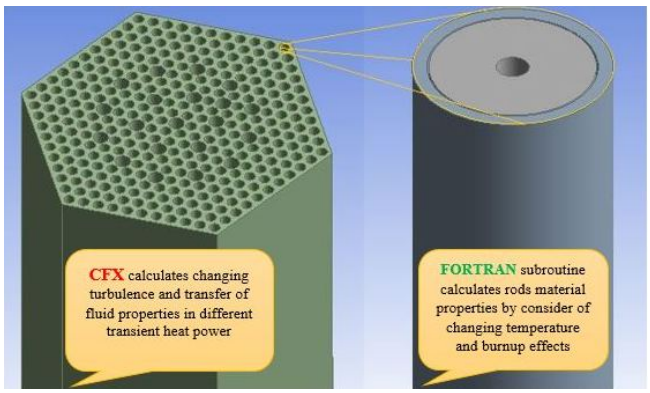


**Figure 1:** Fuel assembly and Fuel rod in simulation.

## 4 Simulation and results

The simulation and results for WWER-1000 in transient are presented in this section. The main properties of this reactor are presented in Table 2. This investigation is performed in two steps: In the first scenario, different amounts of reactivity in various burnups are added to the system and the change in the variables are studied. With the fuel burnup, thermal properties of materials including convection heat transfer coefficient of fuel and the gap are decreased. Hence, it is expected that to create the same thermal flux with more burnup, the system experiences higher temperature. Figure 3 is presented based on the assumption of different burnups of system in constant thermal flux. This figure presents the radial temperature distribution in clad, gap and fuel.

Following the system reactivity in time gives an appropriate justification of the behavior of system. Figure 4 shows the variations of the system reactivity. As can be seen, by adding external reactivity in various burnups, the value of system reactivity changes to zero. These values depend on the initially inserted reactivity and fuel burnup. However, the more the perturbation and burnup, the more the system reactivity. As Fig. 5 shows, by adding negative external reactivity in different burnups to system, the value of thermal power of fuel assembly decreases until it gets steady in a constant value. Finally, and by passing from transient state, the system thermal power has a significant reduction and the system works under a new steady state condition. The previous system properties and conditions are therefore changed.

The average temperature of fuel at the middle section of core is plotted in Fig. 6, and Fig. 7 shows the coolant temperature in the same section. These diagrams not only show the difference between time response of the coolant and fuel and the reactivity changes, but also exhibits that which one predominates the other at the intended step. The fuel temperature at initial time steps is the main effective factor on the response of the system. The effect of the coolant temperature increases over the time; This factor is known as the main effective factor to reach to the stability point again.

Hence, in accordance with Fig. 8, the fuel assemblies were simulated as the fluid inside, and fuel rods were removed. Otherwise, with the aim of decreasing the number of calculations, one sixth of fuel assemblies with a symmetry was chosen, and was considered as the basis for simulation of this part. CFX is able to put these symmetric parts together around an axis and rebuild the whole assembly. Fuel assembly has a specific heat flux profile in axial direction which is presented in FINAL SAFETY ANALYSIS REPORT (FSAR) of Bushehr nuclear power plant. The shape of power distribution along (axial direction) core is in shown in Fig. 9.

Figure 10 shows the velocity vectors of fluid considering the cross flow. These data clarify the maximum velocity of fluid and its location as well. The velocity streamlines are plotted in Fig. 11. As expected, coolant velocity reduces in sticking film on the wall because of friction.

**Table 2:** WWER-1000 Operating Parameters.

| Parameter | Value |
|---|---|
| Reactor heat power (MW) | 3000 |
| The primary pressure at the core outlet (MPa) | 15.7 |
| Steam pressure in the steam header of the steam generator (MPa) | 6.27 |
| Design pressure in the primary circuit (MPa) | 17.6 |
| Design pressure in the secondary circuit (MPa) | 7.84 |
| Temperature at reactor inlet (°C) | 291.0 |
| Coolant flow rate through the reactor ($m^3$/h) | 84800 |
| Effective fraction of delayed neutrons, $10^{-3}$ | 7.4 |
| Engineering safety factor | 1.16 |
| Fraction of coolant flow rate in the channel of leaks (core by-pass) (%) | 4.0 |

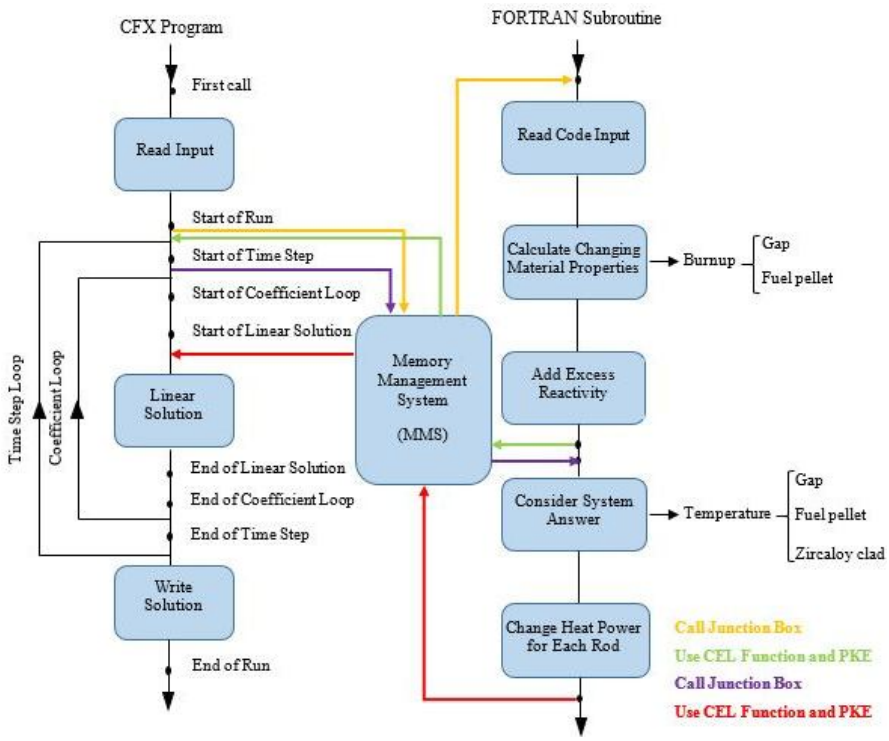


**Figure 2:** The algorithm of coupling FORTRAN subroutines to CFX.

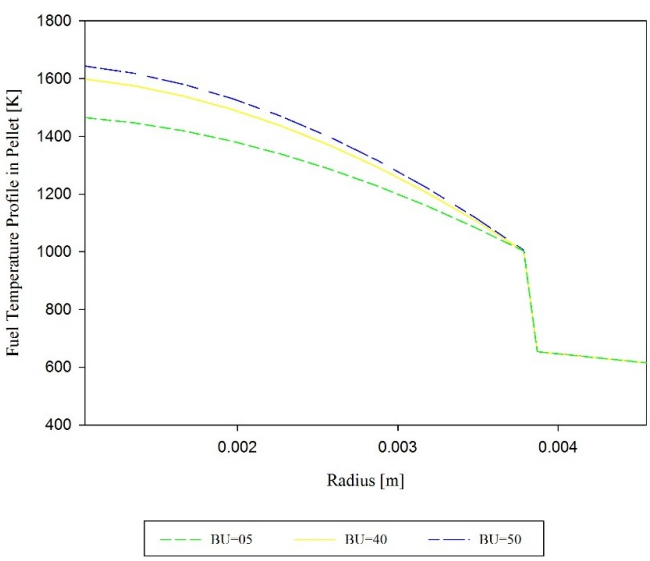


**Figure 3:** Temperature profile of fuel rod in radial direction for different values of fuel burnups.

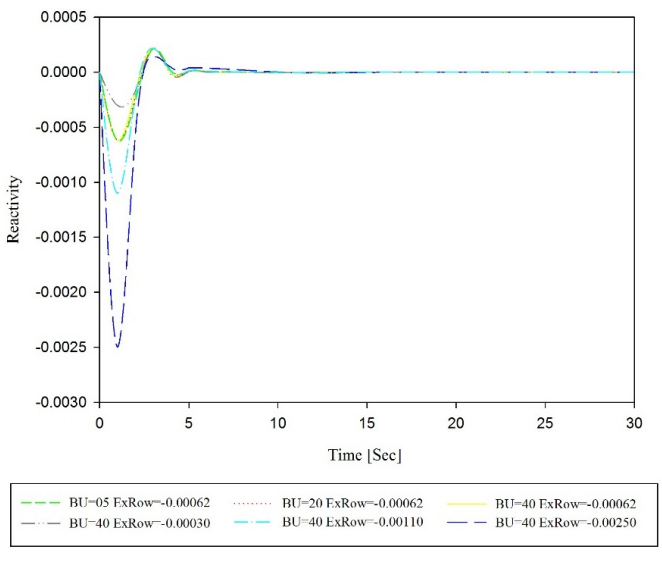


**Figure 4:** Reactivity versus time in different fuel burnups.

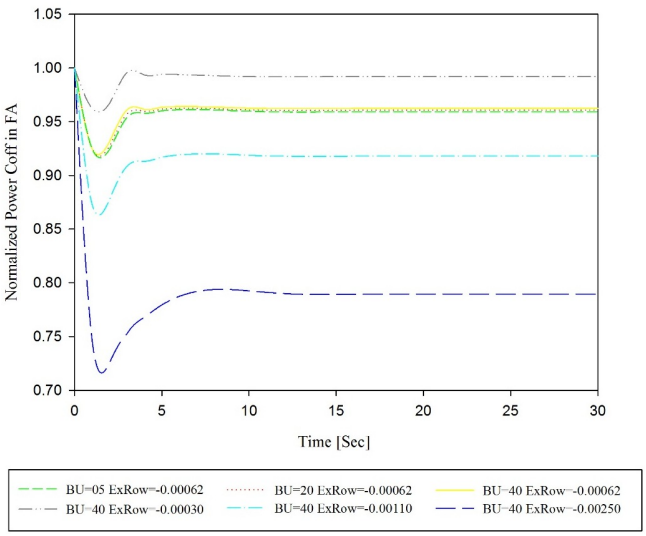


**Figure 5:** Power changes vs time in different fuel burnups.

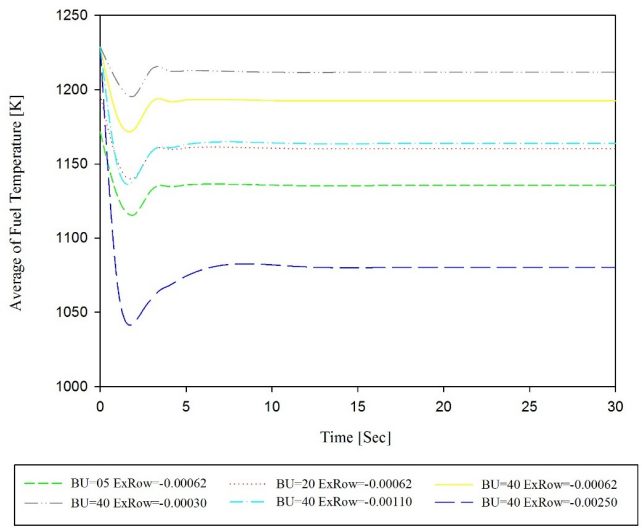


**Figure 6:** The average fuel temperature in middle section in different fuel burnups.

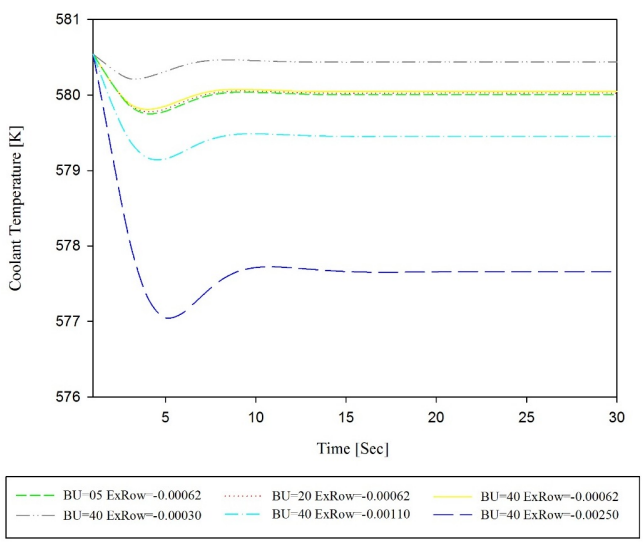


**Figure 7:** The coolant temperature in middle section in different fuel burnups.

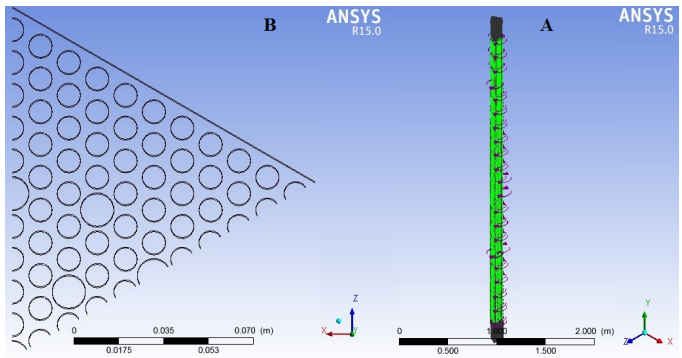


**Figure 8:** One sixth of fuel assemblies, (A) completely, (B) top view.

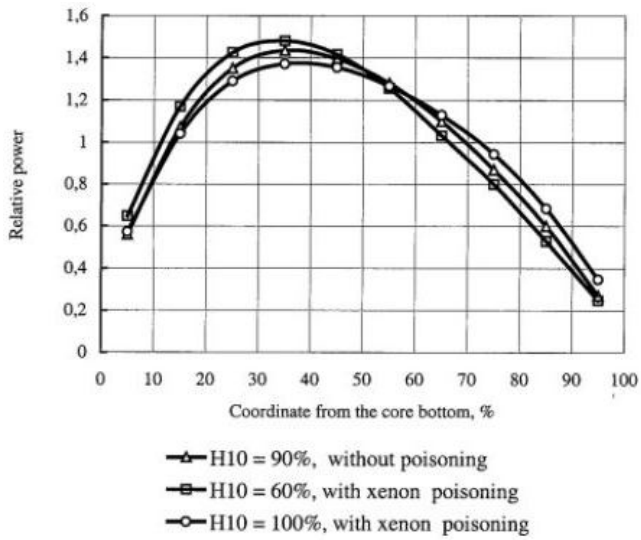


**Figure 9:** Power axial distribution profile (FSAR, 2005).

Figure 12 shows the temperature gradient on the surfaces of the fuel rods. In this situation, the fluid temperature gradient is considerable in the points with high heat powers (See Fig. 9).

Figures 13 and 14 show the fluid temperature in the axial direction for steady state in a fuel assembly. As expected from Bushehr FSAR, fluid temperature increases to 321°C in the outlet.

In the second scenario, for transient analysis in core, the fuel assemblies in core are classified in five categories according to the power peaking factors (See Fig. 15). The steady state results of the core are presented in Figs. 16 and 17.

According to the literature, the average value of burnup in first cycle for each fuel assembly is 12 $\frac{\text{MW.day}}{\text{kgU}}$. Owing to the fact that the value of burnup for each assembly depends on its relative power, fuel burnup and accordingly the constitutive material properties are calculated individually for each group of mentioned assemblies. In the next step, external reactivity in amount of -0.00062 is added to each fuel assembly and their behavior is observed over the time. Figure 18 presents normalized power for external reactivity of -0.00062 in each group of classified fuel assemblies. Figure 19 shows the temperature variations in the outlet over the time.

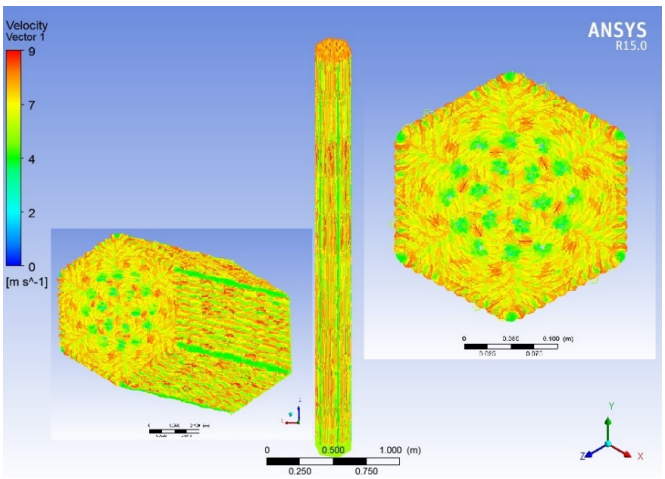


**Figure 10:** Velocity vectors with crossflows.

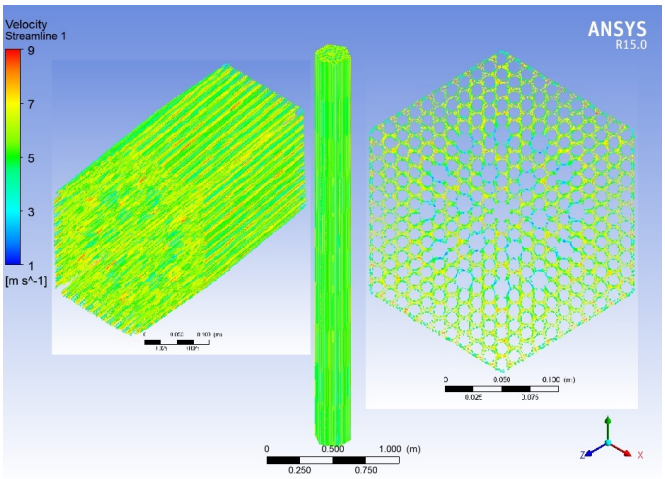


**Figure 11:** Velocity stream lines in fuel assembly.

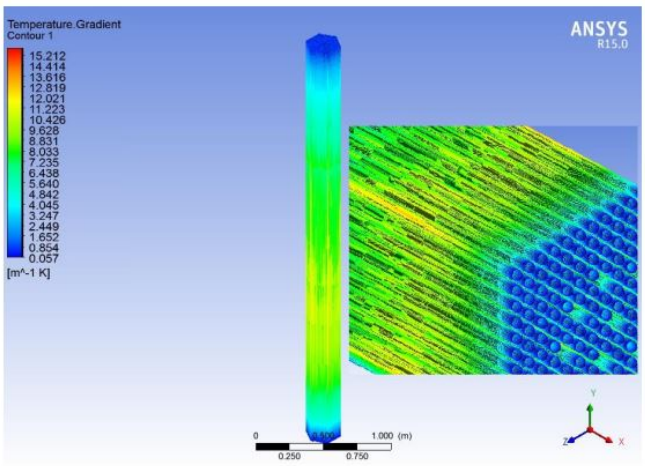


**Figure 12:** Temperature gradient in static boundary film on fuel rods surfaces.

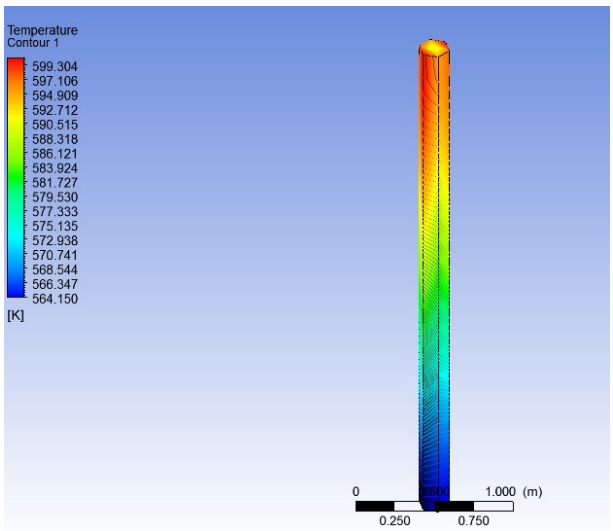


**Figure 13:** Fluid temperature in fuel assembly.

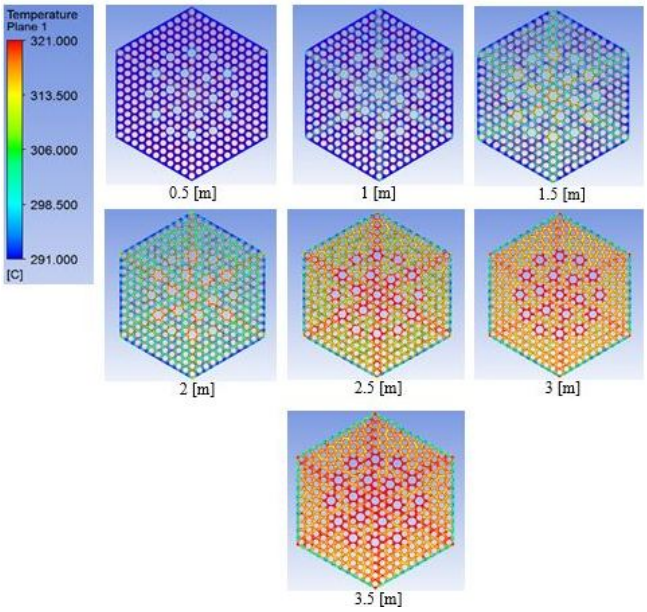


**Figure 14:** Fluid temperature in different heights of a fuel assembly.

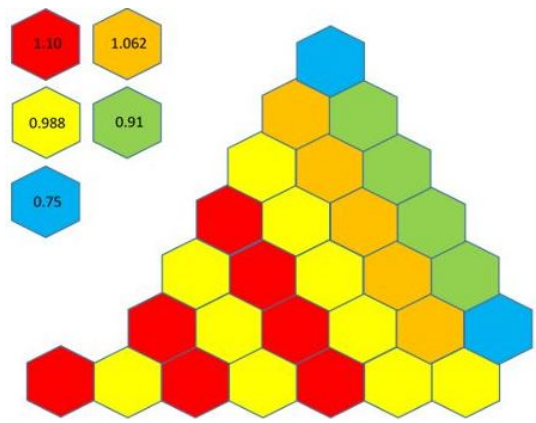


**Figure 15:** Classes of fuel assemblies according to the power peaking factors.

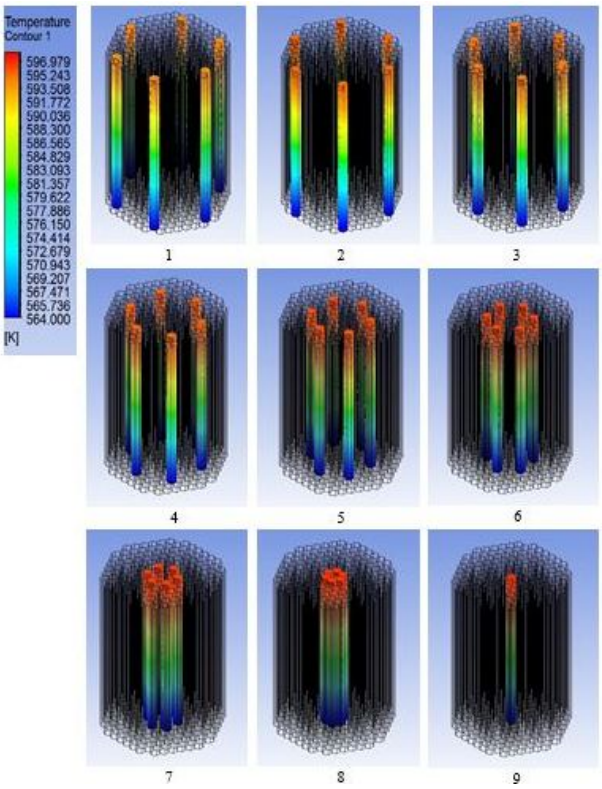


**Figure 16:** Fluid temperature in core.

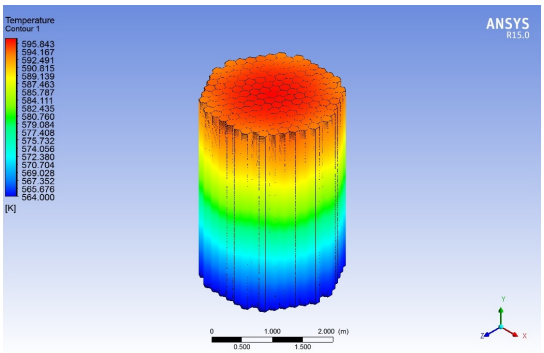


**Figure 17:** Fluid temperature in full core.

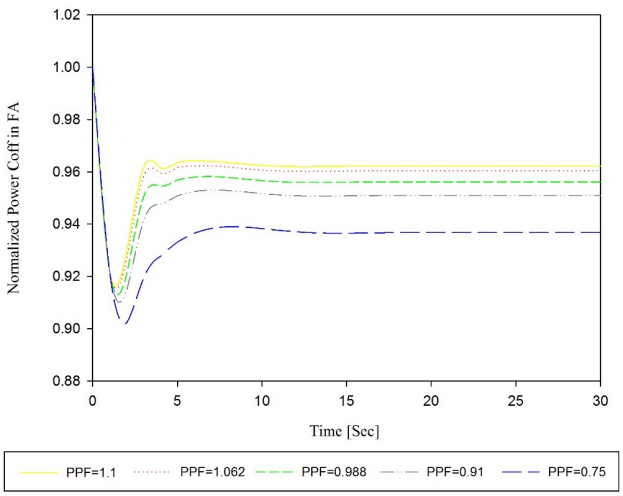


**Figure 18:** Normalized power for various fuel assembly groups with external reactivity of -0.00062.

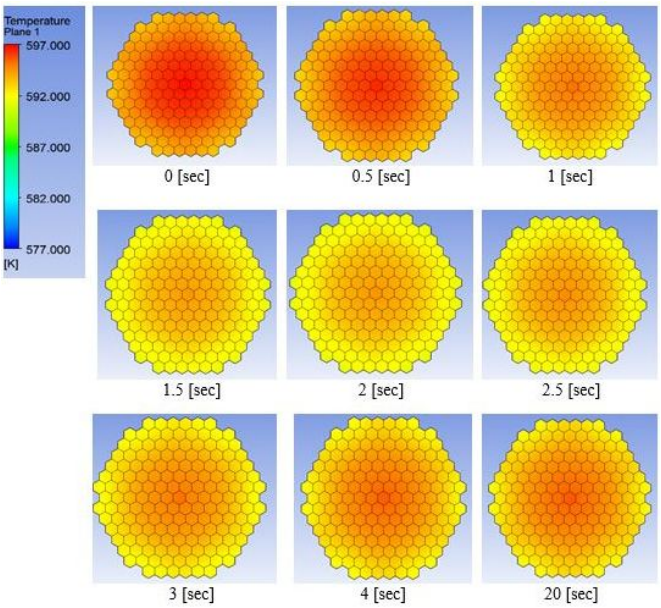


**Figure 19:** Transient temperature of fluid in the outlet of the reactor core.

## 5 Conclusion

In this paper, a coupling method is employed to study the reactivity response of irradiated fuel in transients. In this way, a CFD code is prepared for TH, and the Neutronics power transients are modeled by PKM. In order to evaluate the variation of the fuel rod temperature in transient, a FORTRAN code is prepared and the thermal feedbacks and corrections of the irradiated material properties are considered. All numerical subroutines are coupled to the CFX and memory management system provides data transfer capability.

It has been shown that the irradiated fuels have different responses to the RIAs. The reactivity insertion in several burnups clears that the irradiated fuels show different responses to the same reactivity.

## Acknowledgment

The authors are gratefully indebted to Shahid Beheshti University G. C., for support of this work.

## References

Aghaie, M., Zolfaghari, A., and Minuchehr, A. (2012). Coupled neutronic thermal–hydraulic transient analysis of accidents in PWRs. *Annals of Nuclear Energy*, 50:158–166.

Berna, G. A., Beyer, G. A., Davis, K. L., et al. (1997). Frapcon-3: A computer code for the calculation of steady-state, thermal-mechanical behavior of oxide fuel rods for high burnup. Technical report, Nuclear Regulatory Commission, Washington, DC (United States). Div. of Systems Technology; Pacific Northwest Lab., Richland, WA (United States); Idaho National Engineering Lab., Idaho Falls, ID (United States).

Chen, Z., Chen, X.-N., Rineiski, A., et al. (2015). Coupling a CFD code with neutron kinetics and pin thermal models for nuclear reactor safety analyses. *Annals of Nuclear Energy*, 83:41–49.

FSAR (2005). Final safety assessment report (FSAR) for BNPP. Technical report, Accident Analysis, Book 4, Moscow.

Lucuta, P. G., Matzke, H. J., and Hastings, I. J. (1996). A pragmatic approach to modelling thermal conductivity of irradiated $UO_2$ fuel: review and recommendations. *Journal of Nuclear Materials*, 232(2-3):166–180.

Luyben, W. L. (2012). Use of dynamic simulation for reactor safety analysis. *Computers & Chemical Engineering*, 40:97–109.

Olander, D. R. (1976). Fundamental aspects of nuclear reactor fuel elements: solutions to problems. Technical report, California Univ., Berkeley (USA). Dept. of Nuclear Engineering.

Smith, B. L. (2010). Assessment of CFD codes used in nuclear reactor safety simulations. *Nuclear Engineering and Technology*, 42(4):339–364.

Vyskocil, L. and Macek, J. (2014). Coupling CFD code with system code and neutron kinetic code. *Nuclear Engineering and Design*, 279:210–218.